

DYNAMIC FRACTURE STUDIES OVERVIEW

Zdenek Bilek*

Institute of Physical Metallurgy, CSAV, 61662 Brno
Zizkova 22, Czechoslovakia

*Visiting Professor of Engineering, Centro de Estudios e
Investigaciones Técnicas de Guipúzcoa, B°Ibaeta, s/n
20009 SAN SEBASTIAN. SPAIN

ABSTRACT

The application of a dynamic fracture mechanics approach to the safety assessment of engineering structures requires the availability of relevant data. Namely it is necessary to have information on dynamic fracture toughness K_{Id} associated with rapid loading conditions and on crack propagation fracture toughness K_{ID} . In this paper the influence of loading rate and temperature on K_{Id} is demonstrated up to high loading rates produced by Hopkinson Split Bar Technique. The dependence of K_{ID} on crack velocity was measured for propagating cracks using slowly wedge opened double cantilever beam specimens. Dynamic fracture experiments were performed for three structural steels with ferrite-perlite and bainite microstructures. It is shown that the K_{ID} values are well above the K_{Id} data generated at high crack tip loading rates $K \approx 10^6 \text{ MPam}^{1/2}\text{s}^{-1}$ which therefore represent the minimum fracture toughness.

RESUMEN

La aplicación de la Mecánica de la fractura dinámica, a las valoraciones de seguridad de una estructura de ingeniería, requiere conocer aquellos parámetros relevantes. Fundamentalmente se precisa la tenacidad en función de la velocidad de aplicación de las cargas: K_{Id} , y en función de la velocidad de propagación de la grieta: K_{ID} . Este artículo discute la influencia de la temperatura y la velocidad de carga sobre K_{Id} hasta las velocidades alcanzables con la técnica de barra Hopkinson. La dependencia de K_{ID} sobre la velocidad de propagación fue medida con probetas cargadas mediante una cuña. Los ensayos se realizaron sobre tres aceros con microestructuras ferrítico-perlítica y bainítica. Se concluye que los valores de K_{ID} son claramente superiores a los valores de K_{Id} medidos con altas velocidades de carga $K \approx 10^6 \text{ MPa}\sqrt{\text{m}}/\text{s}$; representan, por tanto, la mínima tenacidad de fractura

INTRODUCTION

The fracture failure of pressurized pipelines, bridge girders, ship hulls, pressure vessels and etc. can be prevented by applying static and dynamic fracture mechanics procedures in the process of calculation, design, materials selection and construction of such structures. Dynamic fracture mechanics plays the important role in quantification the conditions under which a rapid load bearing structure can fail due to the enlargement of a crack contained in that structure or under which a propagating crack will stop before the structural integrity of the unit is lost.

The present paper summarises the recent progress in determination of dynamic fracture properties of three structural steels, while the relevant dynamic mechanical properties were evaluated extensively in [1]. Particular attention is paid to the influence of metalurgical variables, temperature and loading rate K_I on dynamic crack initiation fracture toughness (K_{I_d}) and the influence of microstructure, temperature and crack speed a on crack propagation (K_{I_D}) fracture toughness. The problems related to the used experimental and computational methods are discussed.

For most materials the fracture toughness measured under conditions of impact loading, K_{I_d} , is lower than the static fracture toughness K_{Ic} . Due to rate effects the toughness decreases with increasing loading rate [2]. This behaviour is observed with intermediate loading rates as obtained with the usual instrumented Charpy hammers. But it is not known at present if the same behaviour applies for high loading rates as well. In general there are various possibilities applicable to structural materials as shown in Fig. 1. While the behaviours (a) to (c) are not very realistic since this would imply that K_{I_d} ultimately becomes zero in case (b) or infinity in case (c). The existence of a minimum fracture toughness as in cases (d), (e) is more likely to occur namely for structural steels. A determination as to which behaviour applies can only be made on the basis of experimental K_{I_d} investigations over the broad spectrum of crack tip loading rates K_I .

Direct measurements of the impact fracture toughness at high loading rates have been performed using different experimental techniques including flyer - plate arrangements, electromagnetic forces, projectile impacting and Hopkinson Split Bars Technique (HSBT) in various modifications [3-5]. There is general agreement that an appropriate quantitative form for the initiation of unstable crack growth is given by the equation

$$K_I(t) = K_{I_d}(K_I, T) \quad (1)$$

where K_{I_d} is supposed to be a material property that depends upon the loading rate K_I and temperature T . The dynamic stress intensity factor $K_I(t)$ depends on geometry and loading conditions, and usually must be found numerically.

To stop a crack in a structure requires a dynamic stress intensity factor $K_I(a)$ in the structure and the materials dynamic fracture toughness $K_{ID}(a, T)$ are in agreement with linear dynamic fracture mechanics simple concept

if $K_I(a) < K_{ID}(a, T)$ then no propagation (2)

if $K_I(a) = K_{ID}(a, T)$ then propagation.

Actual quantitative treatments of criterions (2) present difficulties. Rigorous calculations for structures or specimens with finite dimensions require a fully dynamic analysis of $K_I(a)$ [6,7]. Recent studies on various materials [7] indicate the possible types of resistance response to running crack shown in Fig 2. For any given steel, a three-dimensional plot of dynamic fracture toughness, temperature and velocity, is needed to provide a complete characterization of resistance to fast fracture.

The present paper contributes to the scant information available concerning the temperature and crack velocity dependence of K_{ID} values. The experimental procedure relies on slow [7,8] wedging apart the arms of a precracked rectangular double cantilever beam specimens.

MATERIALS INVESTIGATED

The chemical composition of tested steels is given in Table 1 and microstructures are shown in Fig. 3 to 5.

FRACTURE INITIATION UNDER IMPACT

Experimental set up for stress wave loading follows from Fig. 6. WLCT specimen with geometry shown in Fig. 6 is placed between two steel bars. The first loading bar produces a stress pulse $\sigma_I(t)$ with duration time of $\lambda_I = 52\mu s$, $\sigma_T(t)$ is a stress pulse transmitted to the second bar. To evaluate the K_{ID} values we used procedure based on finite element computations for the geometry given in Fig. 6 and ratio $a/w = 0.5$. The problem was treated as plane one. The values of static stress intensity factor K_I^s were determined by means of hybrid technique. For dynamic calculations the program BKDYN [6] was used to solve elastic and elastic-plastic problems. This program makes use of four node quadrilateral elements and for time integration the explicit central difference method is implemented with automatic selection and adjustment of time step. The loading was modelled by real opening force $F(t)$ shown in Fig. 7 and the values of dynamic stress intensity $K_I(t)$ was alternatively found from the crack tip displacements and from the path independent integral computations. It is obvious that the latter approach results in better agreement with supplementary calculations using special crack tip element [9]. The boundary conditions correspond to free surface specimen during the impact loading. Typical results are summarized in Fig. 7 to 9 for mesh having

2500 elements and 2660 nodal points for one half of the specimen.

In addition to the shock wave tests operating with $K_I \approx 10^6$ MPam^{1/2}s⁻¹ also intermediate and low loading rates tests were carried out using standard compact tension specimens loaded by the hydraulic computer operated testing machines ZWICK. All the experiments were performed at wide temperature range (-196 to 20)°C.

The results shown in Fig. 7 indicate a great difference between K_I^s and $K_I(t)$ so one should be very careful evaluating K_{Id} values according the procedures based on static analysis as recommended in reference [4]. Also Fig. 7 suggests that displacement extrapolation is not accurate enough to provide the correct values of $K_I(t)$. The extensive plastic zone development studies in the particular form of Fig. 8 suggest that despite unusually small specimens the plane strain conditions prevail and our K_{Id} data are valid from this point of view. Fig. 9 demonstrates the complicated way of crack tip loading during the test. Figs. 10, 16 show fracture toughness as a function of loading rate and temperature. Both figures show substantial rate effects. This is a very important engineering problem since some designs against fracture should be performed using a minimum expected value of fracture toughness, but its value depends not only on temperature but also on loading rate.

Knott [11] have presented an analysis which related the critical cleavage stress σ_{cf} to K_{Ic} . Essentially this approach was adopted in this paper for K_{Id} interpretation. The cleavage stress σ_{cf} and process zone size R_o over which this stress is reached were found following reference [5]. For example, for steel C, $\sigma_{CF} = 1600$ MPa and $R_o = 0.065$ mm. Assuming that both quantities σ_{cf} and R_o are independent of strain rate and temperature we find with help of Fig. 9 that fracture criterion $\sigma_{yy} = \sigma_{cf}$ is met for $x = R_o$ at time $t = 8 \mu s$. On the other hand at this time the dynamic stress intensity (Fig. 9) reaches the value of $K_I(t) = 6$ MPam^{1/2} which is below $K_{Id} = 20$ MPam^{1/2}. This value of K_{Id} is reached later at $t = 15 \mu s$, which supports the existence of incubation time ($7 \mu s$) proposed in refs. [3] to initiate a fracture by stress pulse loading.

FRACTURE PROPAGATION AND ARREST

The unstable crack propagation study employed RDCB specimens which were slowly wedge loaded as described in [6 to 8]. The experimental set up as installed on a 200 kN Zwick machine is illustrated in Fig. 11. Crack velocity was recorded using crack propagation gauges. The crack velocity was varied by changing the root radius of the starting notch from 0.2 to 1 mm. The blunted notch permits the specimen to sustain a stress intensity K_{Iq} prior to the onset of crack propagation which is greater than the K_{Ic} values. Therefore, as soon as a sharp crack emerges from starting notch, the crack immediately propagates rapidly under constant displacement conditions. During a typical test, a steady-state velocity was maintained from start until shortly before arrest as can be seen from

Fig. 12 where the crack length versus time is shown.

The values of K_{ID} were determined by dynamic finite element analysis using the BKDYN program [6]. Crack propagation was simulated by the gradual release of nodal points. Applying fine finite element breakdown consisting of 600 elements for one half of RDCB specimen the K_{ID} values were calculated from the measured crack velocity profiles. Good agreement between theoretically predicted [7] and measured values of a and K_{ID} is obvious from Fig. 13 for steel B.

The effect of crack velocity on K_{ID} values at selected temperatures is demonstrated in figures 14, 15; a trend toward lower K_{ID} values with increasing fracture velocity is apparent for bainitic steel C. However, the exact form of the K_{ID} - a curves is not clear because of limbo range for crack velocities lower than 500 m/s. Further experimental work using the rapid wedging of RDCB specimens [10] is required to complete the K_{ID} - a dependences. Fig. 16 compares the K_{ID} values with our K_{IC} and K_{Id} measurements made for steel A. The most striking feature of the results is the large difference between the K_{ID} values for a propagating crack, and the dynamic initiation values K_{Id} for a rapidly loaded, but stationary crack. It has generally been thought that K_{Id} values approximate the toughness of propagating cracks. Our K_{ID} are well above the reference fracture toughness curves K_{IR} also drawn in Fig. 16. Crack arrest fracture toughness K_{Ia} gives the lower bound of K_{ID} data -Fig. 16 for all three steels studied.

ACKNOWLEDGEMENT

The author would like to express his gratitude to the CAICYT providing the financial support during his stay in Spain.

REFERENCES

- [1]- J. Buchar, Z. Bilek and F. Dusek, "Mechanical behavior of metals at extremely high strain rates". Trans. Tech. Publication, Aedermamsdorf, Switzerland, 1986.
- [2]- J.F. Kalthoff, "Fracture behavior under high rates of loading", Eng. Fract. Mech. No. 1, 1986.
- [3]- L.S. Costin et al. "Fracture initiation in metals under stress wave loading conditions", G.T. Hahn and M.F. Kanninen, Fast fracture and crack arrest ASTM STP 627, Philadelphia, 1977.
- [4]- J.R. Klepaczko "Loading rate spectra for fracture initiation in metals", Theoret. Appl. Fract. Mech. No. 1, 1984.
- [5]- Z. Bilek et al. "The influence of microstructure and temperature on

static and dynamic fracture initiation in heat resistant steel" J. Carlsson and N.G. Ohson, Mechanical behaviour of materials 2, Stockholm, 1983.

- [6]- Z. Bilek, "Dynamic fracture toughness of a structural steel", D. Francois, Advances in fractures research 2, Cannes, 1981.
- [7]- M.F. Kanninen, C.H. Popelar "Advanced fracture mechanics", Oxford University Press, New York, 1985.
- [8]- G.T. Hahn "Fast fracture toughness and crack arrest toughness" G.T. Hahn and M.F. Kanninen, "Fast Fracture and Crack Arrest", ASTM STP 711. Philadelphia, 1978.
- [9]- C. Atkinson, J.M. Bastero and I. Miranda "Path Independent integrals in Fracture Dynamics using auxiliary fields", Eng. Fract. Mech. No. 5, 1986.
- [10]-S.J. Burns and Z. Bilek "The dependence of the fracture toughness of mild steel on temperature and crack velocity" Met. Trans. No. 4, 1973.
- [11]-J.F. Knott and Y. Hagiwara "Cleavage fracture in mixed microstructures" D. Francois, Advances in Fracture Research 1, Cannes, 1981.

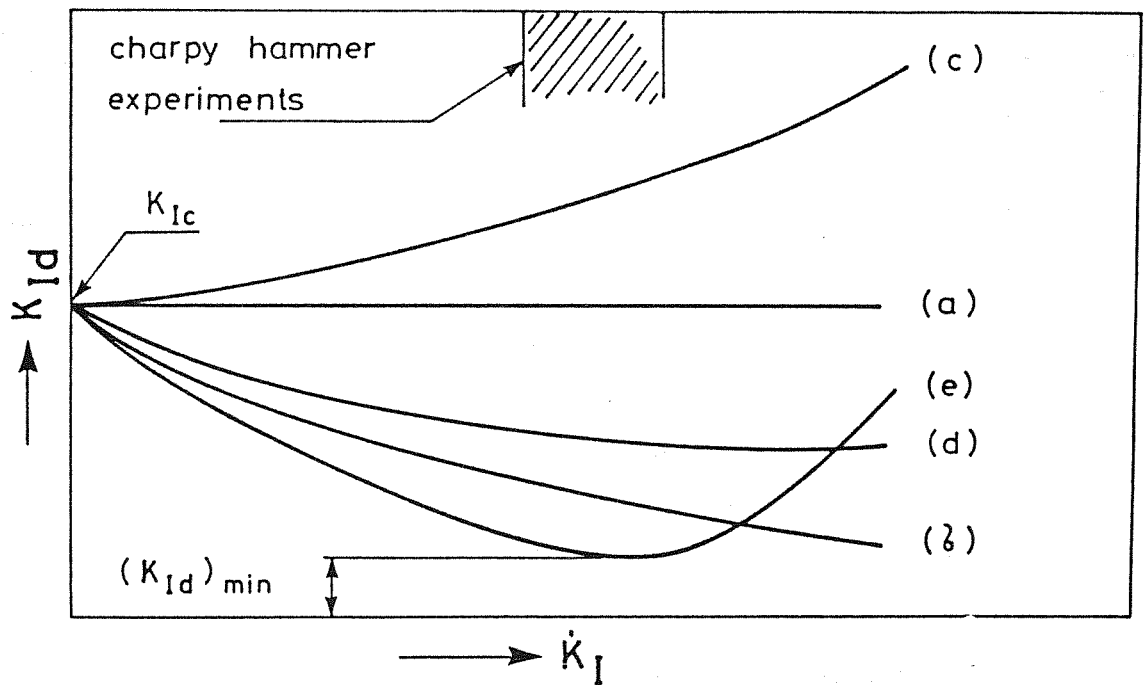


Fig. 1 - Possible behaviour of impact fracture toughness K_{ID} on loading rate \dot{K}_I .

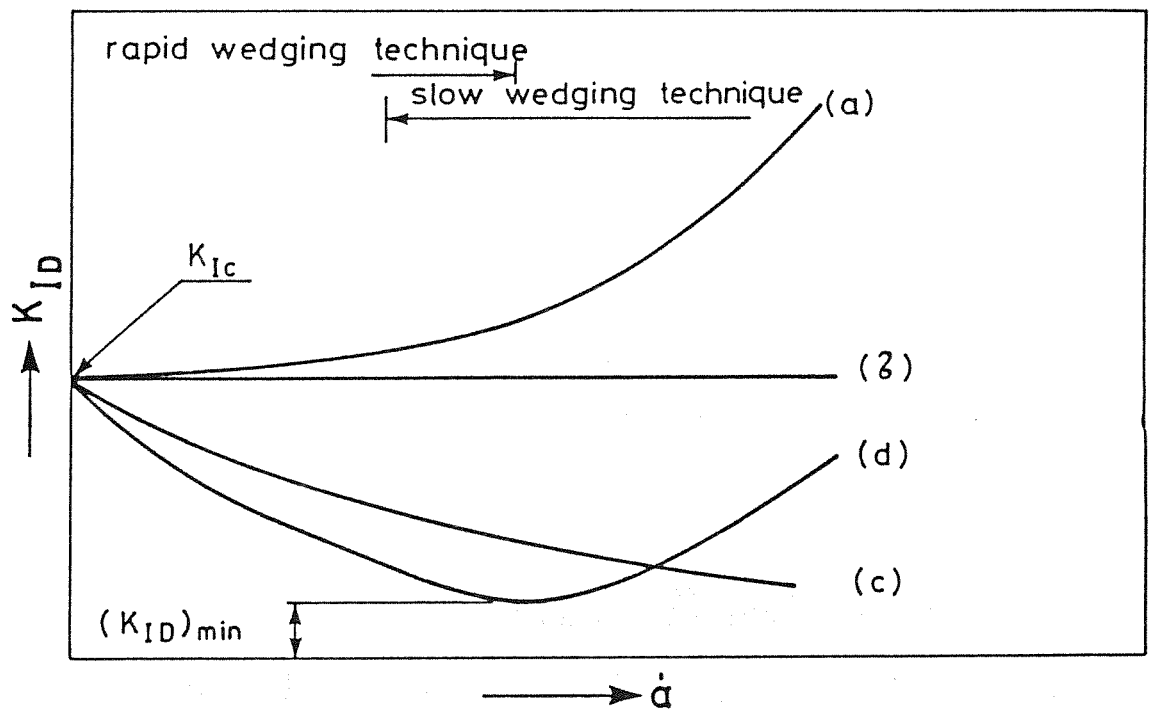


Fig. 2 - Possible behaviour of dynamic crack propagation toughness K_{ID} on crack velocity \dot{a} .

Table 1. The chemical composition of steels.

Steel	C	Mn	P	S	Si	Ni	Cr	Mo	Cu	Al	Ti	N
A	0,19	0,43	0,014	0,016	0,23	-	-	-	-	-	-	0,0055
B	0,20	1,25	0,027	0,022	0,37	0,03	0,10	-	0,06	0,038	0,11	0,0076
C	0,13	0,61	0,010	0,007	0,28	0,22	2,39	0,95	0,05	-	-	-

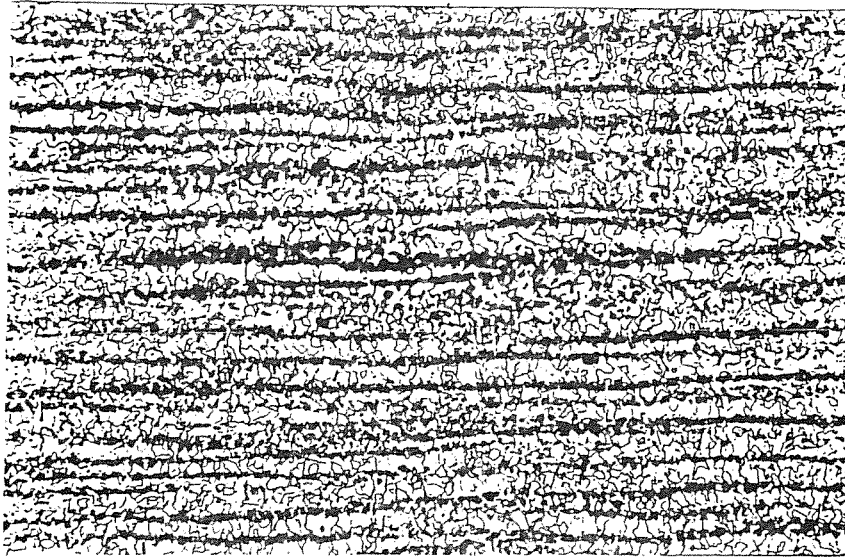


Fig. 3 - Ferrite-perlite microstructure of steel A, 500X.

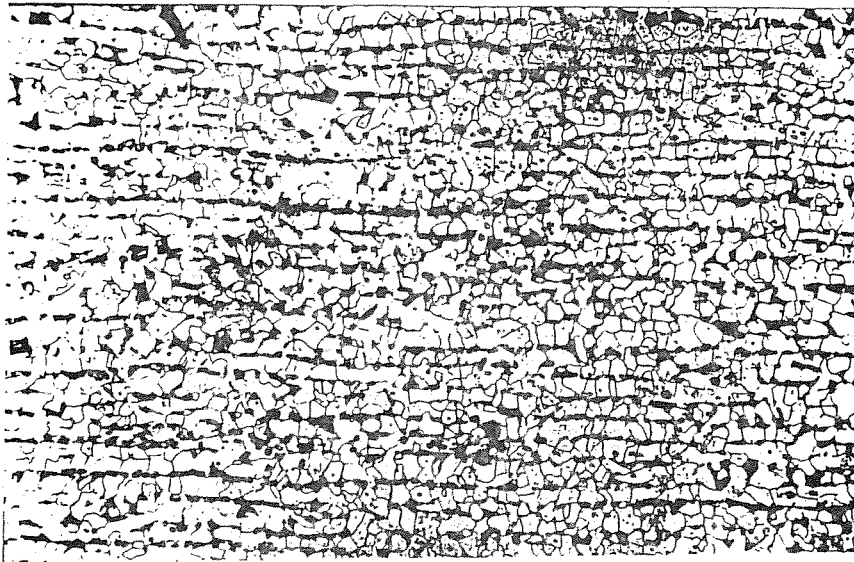


Fig. 4 - Ferrite-perlite microstructure of steel B, 500X.

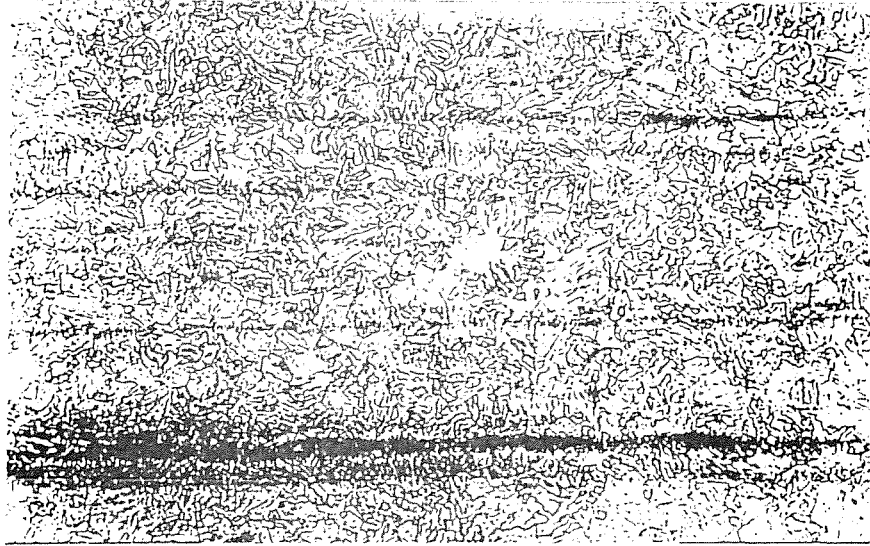


Fig. 5 - Upper bainite microstructure of steel C, 500X.

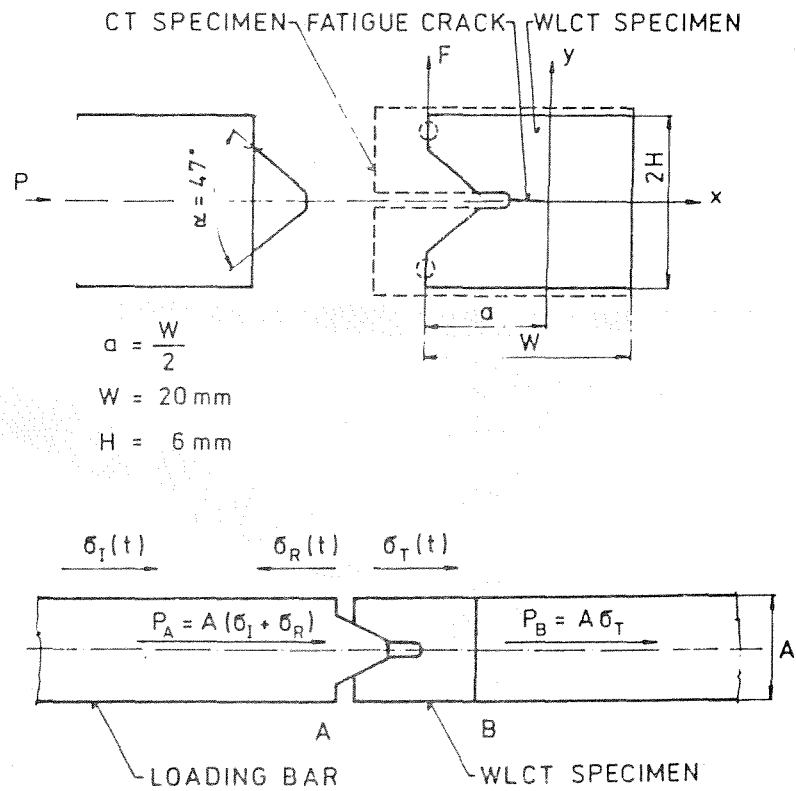


Fig. 6 - Schematic experimental set up for K_{Id} measurements at high loading rates.

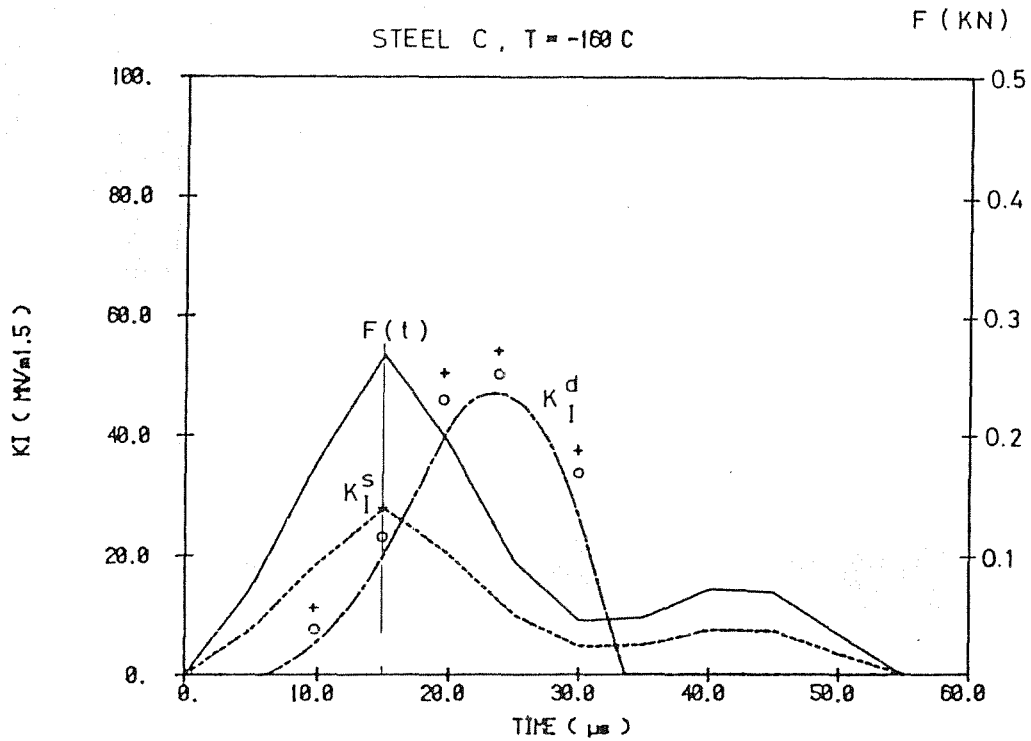


Fig. 7 - Static K_I^S , dynamic K_{Id} /9/ stress intensity factor and loading pulse per lmm thickness $F(t)$ vs. time.
 + Displacement extrapolation
 o Path independent integral computations.

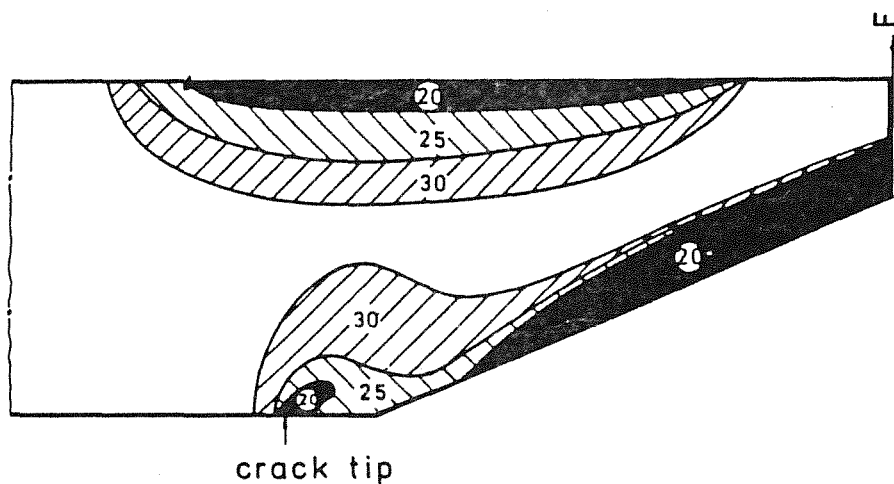


Fig. 8 - Plastic zone development for 20,25 and 30 us for linear hardening with secant modulus $E/165$.

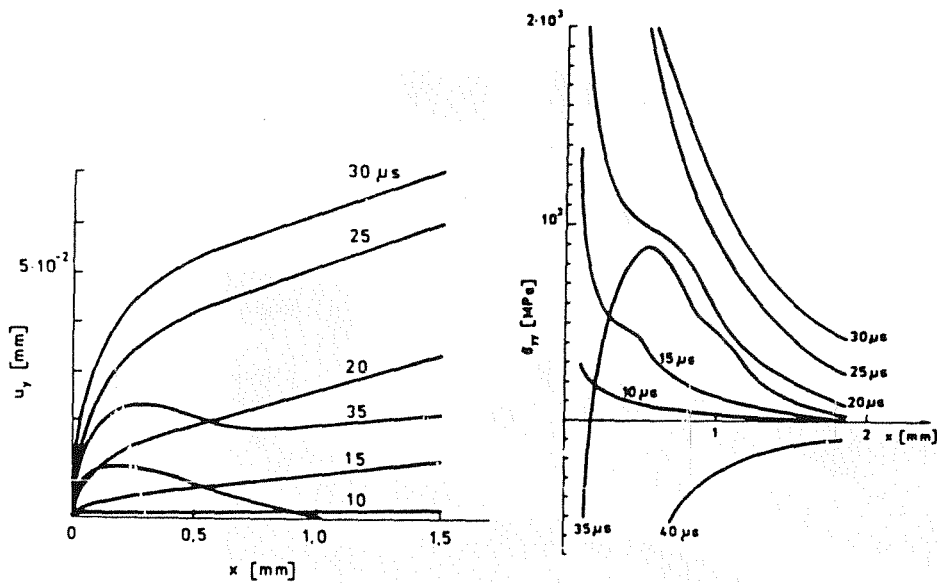


Fig. 9 - Normal stress σ_{yy} behaviour at the crack tip and crack profiles.

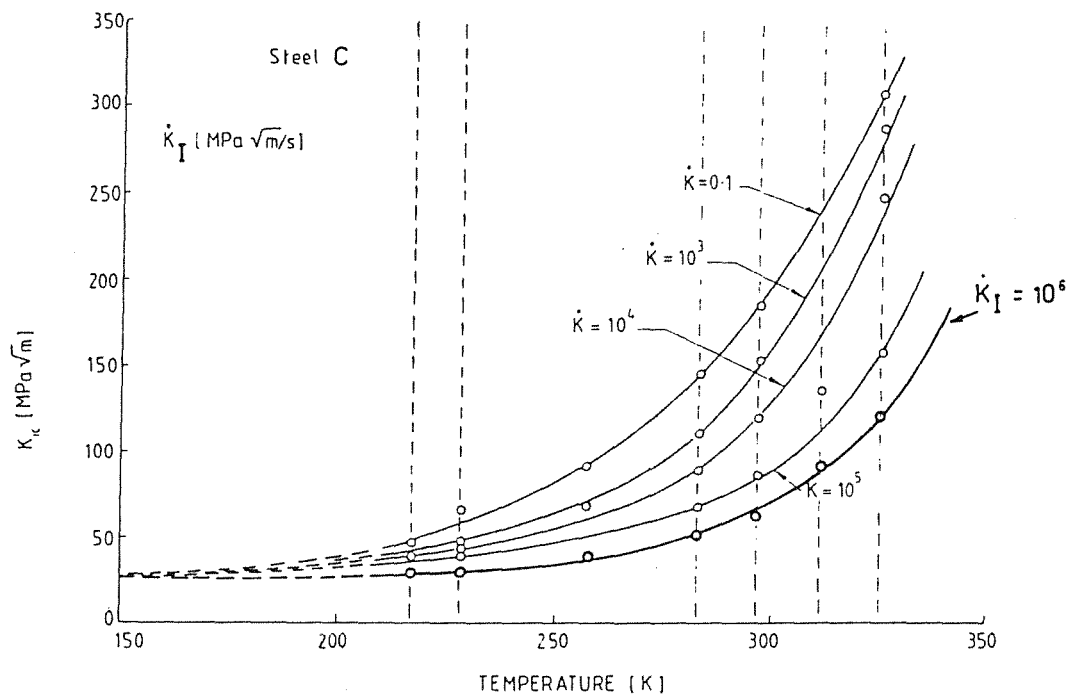


Fig. 10 - Fracture toughness as a function of loading rate \dot{K}_I .

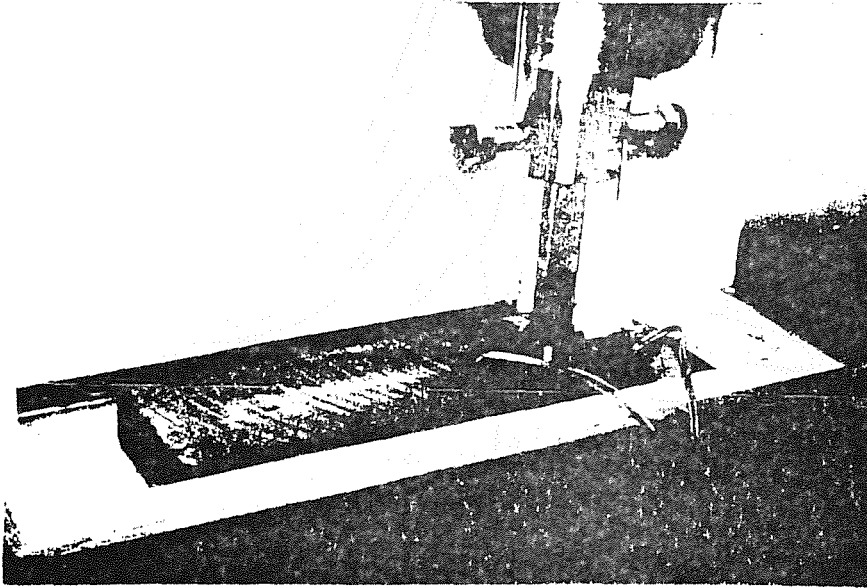


Fig. 11 - Transversal wedge loading test arrangement.

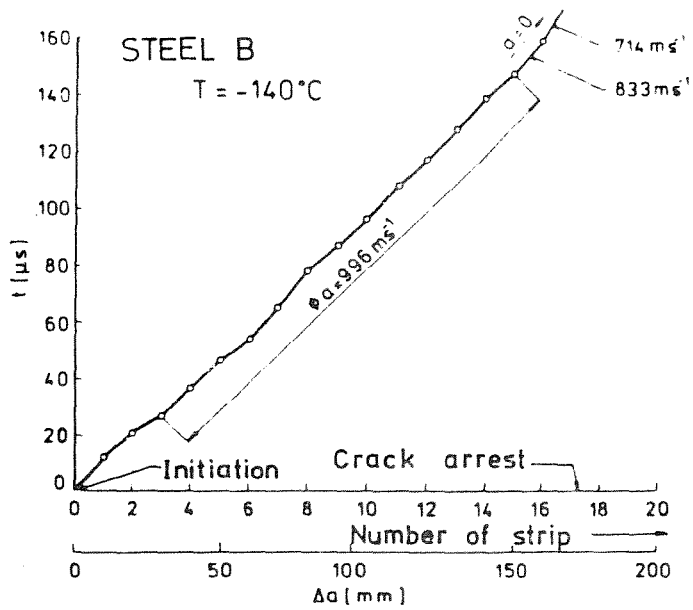


Fig. 12 - Crack length, a-time, t history, steel B.

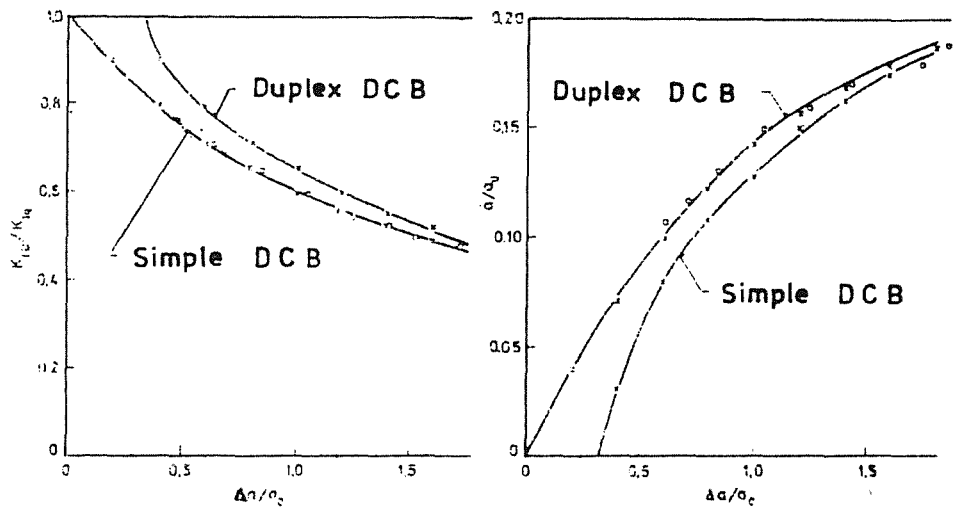


Fig. 13 - Relation between crack length, K_{ID} and crack speed \dot{a} .
 x - fem calculations,
 o - experimental measurements, steel B.

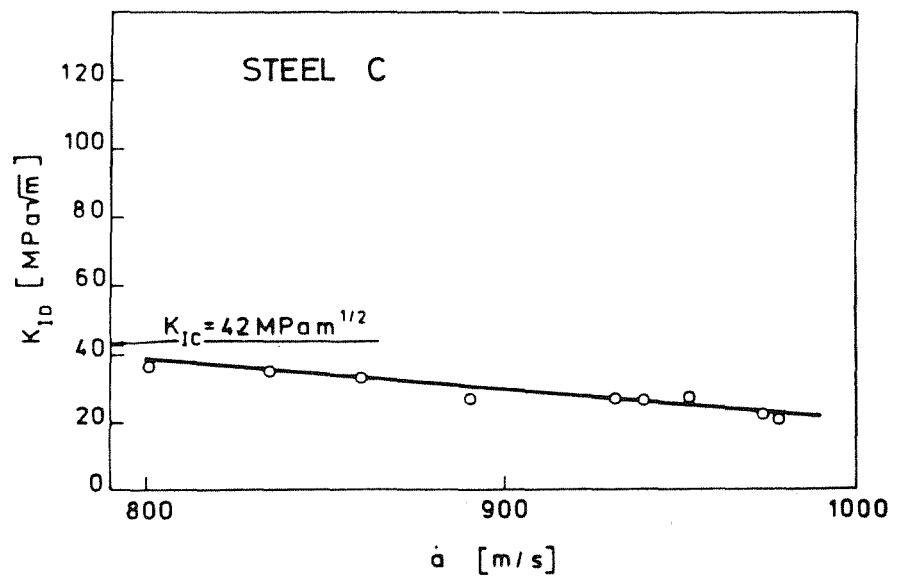


Fig. 14 - K_{ID} - \dot{a} curve for steel C at $T=-160^{\circ}\text{C}$.

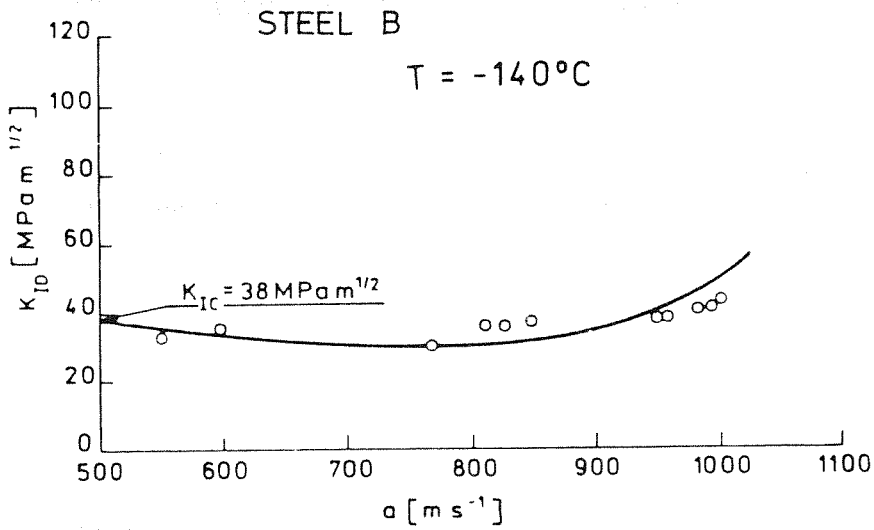


Fig. 15 - K_{ID} - \dot{a} curve for steel B at $T=-140^{\circ}\text{C}$.

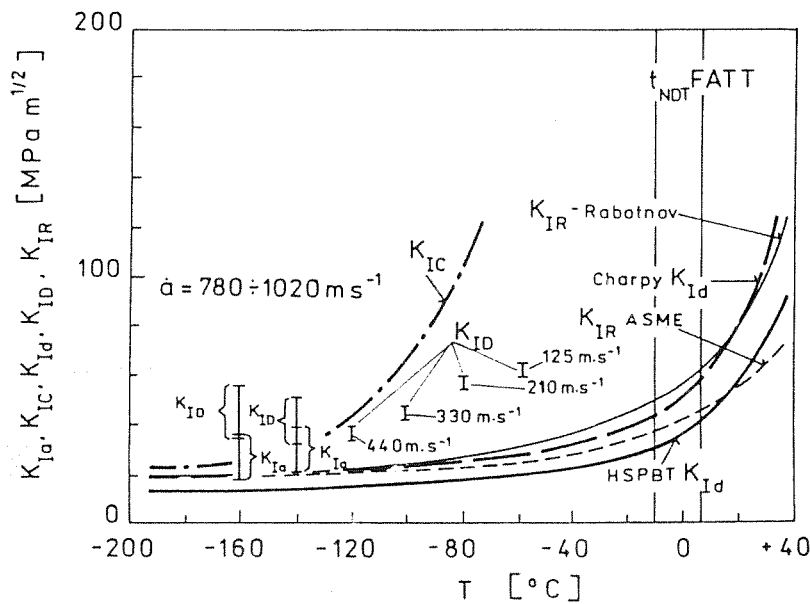


Fig. 16 - Temperature dependence of fracture toughness, steel A.